Journal of Applied Polymer Science

UV-Activated Silicone Oligomer Cross-Linking Through Photoacid and Photobase Organocatalysts

Abraham Chemtob,[1] Héloïse De Paz-Simon,[1] Céline Croutxé-Barghorn,[1] Séverinne Rigolet[2]

[1]Laboratory of Macromolecular Photochemistry and Engineering, University of Haute-Alsace, ENSCMu, 3 rue Alfred Werner, 68093 Mulhouse Cedex, France

[2]Institute of Mulhouse Material Science, Equipe Matériaux à Porosité Contrôlée, UMR-CNRS 7361, University of Haute-Alsace, 3 rue Alfred Werner 68093, Mulhouse Cedex, France

Correspondence to: A. Chemtob (E-mail: abraham.chemtob@uha.fr)

ABSTRACT: Diphenyl iodonium hexafluorophosphate salt and *N*-alkyl morpholino acetophenone were shown to be effective photocatalyst generators for the cross-linking of α,ω-silanol terminated silicone oligomers. These two photoacid and photobase-induced polycondensation pathways provided an attractive and efficient alternative to toxic and expensive organometallic catalysts. The utility of this novel UV-curing process was demonstrated with a combination of time-resolved infrared spectroscopy to follow the fast reaction kinetics and solid-state ^{29}Si nuclear magnetic resonance to investigate the polysiloxane network. © 2013 Wiley Periodicals, Inc. J. Appl. Polym. Sci. **2014**, *131*, 39875.

KEYWORDS: photopolymerization; crosslinking; coatings; photochemistry; polycondensation

Received 9 July 2013; accepted 15 August 2013

DOI: 10.1002/app.39875

INTRODUCTION

The versatility of silicone materials has enabled them to penetrate many varied consumer markets as sealants, release coatings, mold-making elastomers, biocompatible medical devices, or dielectric coatings.[1] For all these applications, a reticulated elastomeric microstructure is essential, and can be achieved in most cases via the cross-linking of low-molecular-weight fluid oligomers based on polydimethylsiloxane (PDMS).[2,3] Conventionally, curing is carried out through Pt or Rh catalyzed-hydrosilylation reactions with a heated two-part product including SiH- and vinyl-functionalized PDMS.[4,5] The second well-established route implies organometallic Sn salt or Ti alkoxide catalysts for the condensation of hydroxyl end-blocked PDMS with moisture-sensitive silane cross-linkers such as alkoxysilane or acetoxysilane.[6] Only when exposed to atmospheric moisture does the silane derivative hydrolyze, and the resulting silanol groups can subsequently condense with the OH-PDMS chains at room temperature to form a siloxane network. Whilst these two cross-linking technologies are well-accepted industrially, the use of organometallic catalysts raises many issues.[7] Their cost, complexity of synthesis, toxicity, and in some cases sensitivity to water provide motivation to devise novel cross-linking methods involving simple catalysts. In addition, the elimination of metal residues from the final silicone product could be highly desirable in biomedical or microelectronic applications.[8]

Herein, we demonstrate the high activity of two alternative acid and base organic photocatalysts for the cross-linking of films based on α,ω-silanol terminated silicone oligomers (Scheme 1). Under UV-irradiation, the decomposition of a diaryl iodonium salt (**1**)[9] and a α-aminoketone (**2**)[10] *in situ* generates respectively $H^+PF_6^-$ and tertiary amine acting as efficient condensation catalysts. The interest in iodonium salts is mainly due to their very useful reactivity, combined with benign environmental character and commercial availability. Onium salts photoacid generators (PAG) such as **1** have been widely reported in lithography and cationic photopolymerization,[11,12] while the α-aminoketone photobase generator (PBG) **2** has found particular use in sol–gel reaction[13] and epoxy-carboxylic acid nucleophilic addition.[14,15] Our UV-driven approach is significantly different from previous photocuring methods based on addition photopolymerization of acrylate-[16], epoxy-based[17,18] PDMS or using thiol-ene reaction.[19] In our procedure, photoinduced condensation of OH-PDMS oligomers is performed in presence of a polydimethoxysiloxane oligomeric precursor to afford a cross-linked polymeric structure, as shown in Scheme 2. The use of organic photoacid or photobase enables fast curing rates, an excellent temporal control of the cross-linking reaction, and insensitivity to moisture in absence of UV light. The utility of this novel UV-curing route for the preparation of cross-linked silicone films was demonstrated with a combination of time-resolved infrared spectroscopy to follow the condensation kinetics and

Additional Supporting Information may be found in the online version of this article.

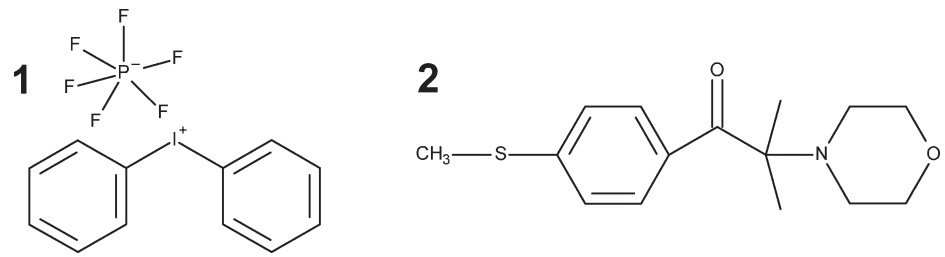

Scheme 1. Diphenyl iodonium hexafluorophosphate salt (**1**) and α-aminoacetophenone (**2**) serving respectively as photoacid and photobase generator.

solid-state ^{29}Si nuclear magnetic resonance to characterize the resultant polysiloxane network.

EXPERIMENTAL

Chemicals

Hydroxyl-terminated poly(dimethylsiloxane) (OH-PDMS, $M_n \sim$ 550 g/mol) was provided by Sigma Aldrich. Polydimethoxysiloxane (PDMOS) behaving as a silicone cross-linking agent is a nonvolatile methoxy siloxane oligomer purchased from ABCR. Full condensation of PDMOS gives on ignition SiO_2 equivalent to 51 wt %, which corresponds to an average of five silicon atoms per oligomer. PDMOS full structural characterization was provided in an another publication.[20] The PAG is a diphenyl iodonium hexafluorophosphate salt (**1**, Sigma Aldrich). The PBG is methyl-1[4-(methylthio)phenyl]-2-morpholinopropan-1-one (**2**, BASF). This α-aminoacetophenone molecule serving as a photobase generator was systematically used in association with benzophenone (BP, 99 wt %) and triphenylphosphine (TPP, 99 wt %) provided by Sigma Aldrich. All chemicals were used without further purification.

Photoinduced Cross-Linking of OH-Terminated PDMS Films

A variable content of PDMOS methoxysilane cross-linker (25–100 wt %) was added to the OH-PDMS. Under photoacid conditions, **1** was subsequently dissolved to the reactive mixture while in a typical photobase-catalyzed condensation process, a **2**/BP/TPP photocatalytic mixture replaced **1**. In each instance, 2 wt % of **1** or 2/2/2 wt % of **2**/BP/TPP with respect to total reactive compounds (OH-PDMS or OH-PDMS/PDMOS) was chosen. Liquid photolatent films exhibiting a thickness of 5 μm were deposited on glass or BaF_2 window using a bar coater, and the film thickness was checked by profilometry measurements. IR transparent BaF_2 pellets were preferred in real-time Fourier transformed infrared (RT-FTIR) experiments in which the samples were simultaneously UV irradiated and analyzed by an IR beam. In this case, the films were irradiated at room temperature by the polychromatic light of a mercury-xenon lamp (Hamamatsu, L8251, 200 W) fitted with a 365 nm reflector, at a constant light intensity of 200 mW/cm^2. The coupling of the lamp with a flexible light-guide enabled a focused illumination of the sample. For samples devoted to solid-state NMR analysis, larger samples were produced through the use of an industrial conveyor, thus showing the possible scaling-up of our procedure. In this second case, the films were placed at room temperature under a UV conveyor with a belt speed of 10 m/min using a microwave powered mercury vapor lamp (H bulb, Fusion). The belt speed of the conveyor was set at 10 m/min and the lamp intensity at 100 %. In these conditions, the emitted light dose for each pass was 1.46 J/cm^2 (UV_A [320–390 nm]: 0.45 J/cm^2, UV_B [280–320 nm]: 0.42 J/cm^2, UV_C [250–260 nm]: 0.09 J/cm^2 and UV_V [395–445 nm]: 0.5 J/cm^2). The samples were subjected to 10 successive passes. During the UV irradiation, the relative humidity was maintained in both cases between 27 and 33% to ensure reproducibility between experiments.

Characterization

Time-resolved transmission infrared spectra were obtained in RT-FTIR experiments with a Bruker Vertex 70 spectrophotometer equipped with a liquid nitrogen cooled mercury−cadmium-telluride detector. All spectra were baseline corrected prior to integration with the software OPUS 6.5. The decay of the IR bands at 2840 cm^{-1} (corresponding to CH_3 symmetric stretch in Si-O-CH_3) was monitored to evaluate the hydrolysis conversion during irradiation time. The percentage of reacted methoxysilyl functions throughout the hydrolysis reaction is obtained by the equation: $C(\%)=100\times\left(\frac{A_0-A_t}{A_0}\right)$ where A_0 and A_t are the area of the absorption band (2840 cm^{-1}) at $t=0$ (before irradiation) and t, respectively.

Before UV irradiation, all liquid film thicknesses were assessed with a profilometer Altisurf 500 workstation (Altimet) equipped with a 350 μm AltiProbe optical sensor. ^{29}Si solid state NMR spectra were obtained by performing Cross Polarization Magic Angle Spinning (CP-MAS) experiments at room temperature on a Bruker Avance II 400 spectrometer operating at 79.49 MHz with a Bruker double channel 7 mm probe. Spectra were recorded using a recycling delay of 5 or 10 s -depending of ^{1}H spin lattice relaxation times (t_1) estimated with the inversion-recovery pulse sequence-, a spinning frequency of 4 kHz and a contact time of 4 ms. ^{29}Si chemical shifts are relative to tetramethylsilane. Peak ratio deconvolution of the various siloxane subspecies was performed with Dmfit software.[21]

The designation D^n and Q^n, respectively, are commonly used in ^{29}Si NMR to describe di- and quaternary coordination of oxygen around silicon. D^n refers to a silicon connected to two oxygens and two organic groups (in the case of PDMS, two methyl groups). The polymer backbone of the silicone oligomer is predominantly D i.e., [$SiO_2(CH_3)_2$]. D^0 ($Si(OH)_2(CH_3)_2$), D^1 ($Si(OH)(OSi)(CH_3)_2$), and D^2 ($Si(OSi)_2(CH_3)_2$) are the three possible structures.

By contrast, the structure of polydimethoxysiloxane (PDMOS) is reflected by Q^n species, which refer to silicon connected to

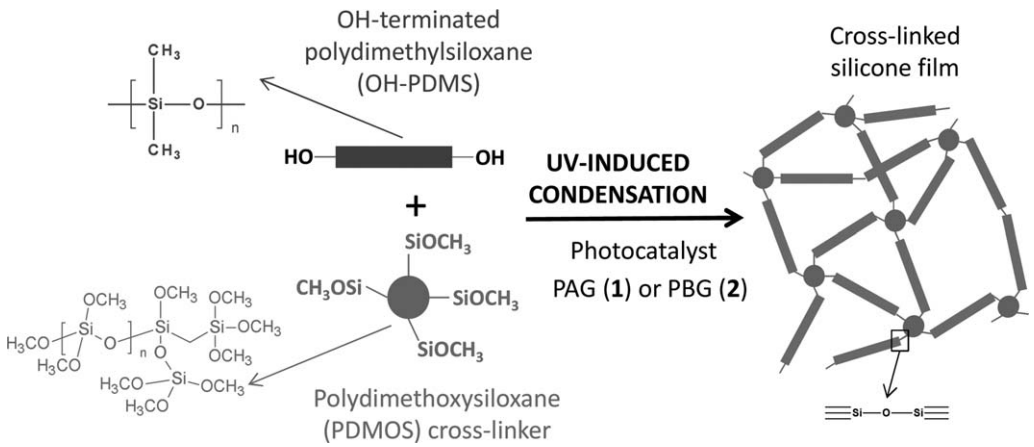

Scheme 2. Photoinduced cross-linking of α,ω-silanol terminated silicone oligomers in presence of polydimethoxysiloxane.

four oxygens. In both cases, the superscript n denotes the number of siloxane bonds. In Q^n species, n ranges from 0 (no siloxane) to 4 (four siloxane bonds). Considering fully hydrolyzed structures, Q^4 ($Si(OSi)_4$), Q^3 ($Si(OSi)_3(OH)$), Q^2 ($Si(OSi)_2(OH)_2$), Q^1 ($Si(OSi)(OH)_3$), and Q^0 ($Si(OH)_4$) sub-species can be found.

RESULTS AND DISCUSSION

Photoinduced Homocondensation of α,ω-Silanol Terminated PDMS

Initially, the weight ratio of **1** and **2** was fixed at 2 wt % with respect to silanol-functionalized PDMS oligomer. 5 μm thick films were cast and irradiated without additional alkoxy cross-linker to evaluate the catalytic activity of the resultant photogenerated acids and bases. Under these conditions, only linear intermolecular homocondensation of terminal SiOH took place to yield longer PDMS chains. The fast chain extension was followed in situ by time-resolved FTIR using the broad OH stretching band at 3400 cm^{-1} as a qualitative marker of the silanol condensation. Utilizing **1** as catalyst, the progressive and full consumption of the SiOH functions was proved by a series of FTIR spectra taken (Figure 1) showing the full disappearance of the OH stretching band within 2 min of irradiation. More specific of silanol is a strong band due to Si-O stretching vibrations occurring at 910 cm^{-1}, whose evolution was found to coincide precisely with that of the OH band. As expected, UV irradiation did not affect the asymmetric and symmetric CH_3 stretching bands at 2900 and 2960 cm^{-1}. By contrast, substantial changes were observed for the asymmetric Si-O-Si stretching vibration in the region 1000–1200 cm^{-1}, whose shape is known to be dependent on polysiloxane structure. Initially viewed as a broad singlet, the UV exposure caused its separation into a doublet pattern with absorbance maxima at 1020 and 1100 cm^{-1} suggestive of an increase in molecular weight.[22] Replacement of **1** by photocatalyst **2** provided no difference in the general temporal evolution of the IR spectra (refer to the Supporting Information Section, Figure S1). In each instance, the conversion-time plot was determined by monitoring the integrated absorbances of the OH stretching mode (3400 cm^{-1}). As displayed in Figure 2, a full conversion was achieved irrespective of the photocatalyst used. However, the photoacid-catalyzed condensation proceeded more rapidly, achieving 100% consumption within 2 min while 10 min were necessary under photobase conditions. Although different reaction mechanisms occurred depending on the catalyst, the higher activity of Brönsted superacids compared to tertiary amines of weak nucleophilicity was somewhat expected. Furthermore, the photobase system required a photosensitizer (benzophenone) as well as an oxygen scavenger (triphenylphosphine)[23] to promote the SiOH condensation within several minutes.[24] A separate infrared study investigating the role of each component of this photobase generator system is included in the supporting information section (Supporting Information Figure S2).

Photoinduced Cross-Linking of OH-Terminated PDMS

Kinetic Aspects. To generate cross-linked silicone film, a series of OH-PDMS photopolymerizations were conducted in presence of polydimethoxysiloxane (PDMOS), a liquid methoxy siloxane oligomer acting as a cross-linker. Using different PDMOS/OH-PDMS weight ratios (0.25 - 1) and photocatalyst (**1** and **2**), transparent and insoluble cross-linked films were achieved each time. Further confirmation of cross-linking was

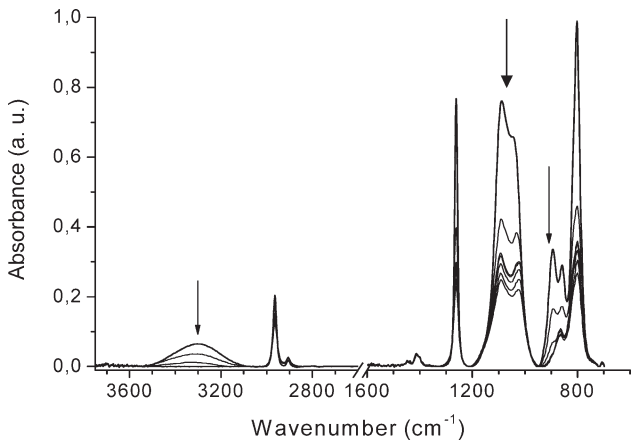

Figure 1. Series of FTIR spectra at six different irradiation times (0, 20, 40, 60, 80, 100, and 120 s) during the UV-triggered OH-PDMS condensation. Film thickness = 5 μm, [OH-PDMS] : [**1**] = 1 : 0.02 (weight ratio), 25°C, Hg-Xe lamp, 200 mW/cm^2, 2 min.

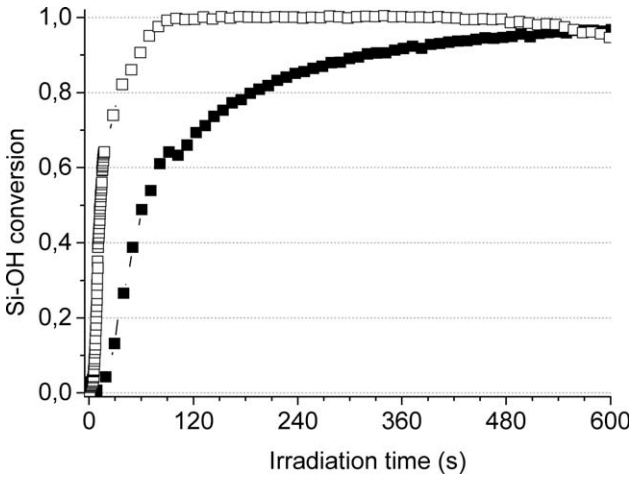

Figure 2. Conversion vs. irradiation time demonstrating the full consumption of the OH-PDMS films in presence of **1** (open symbols) and **2** (full symbols). Film thickness = 5 μm, [OH-PDMS] : [**1**] = 1 : 0.02 (weight ratio), [OH-PDMS] : [**2**] : [BP] : [TPP] = 1: 0.02 : 0.02 : 0.02, 25°C, Hg-Xe lamp, 200 mW/cm^2, 10 min.

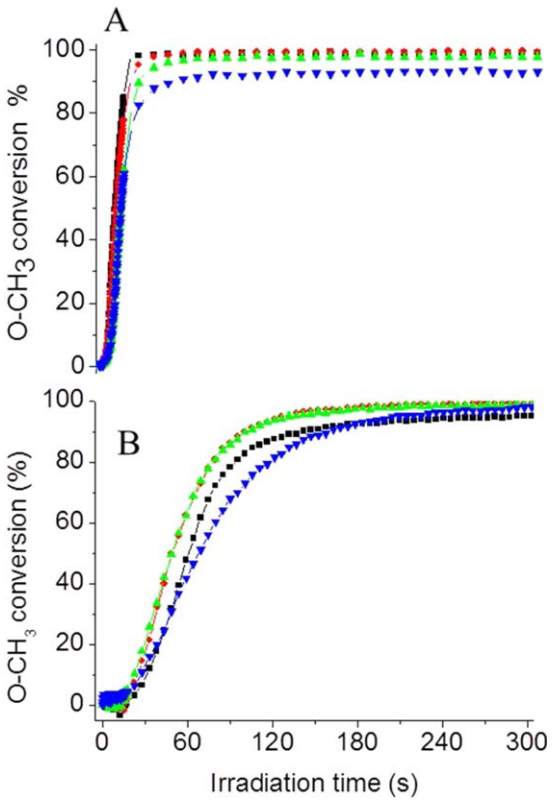

Figure 3. Hydrolysis conversion vs. time during the photoinduced condensation of OH-PDMS catalyzed by **1** (A) and **2** (B) using different weight ratios (x) in PDMOS cross-linker: (▼, 0.25), (▲, 0.50), (●, 0.75), and (■, 1). Film thickness = 5 μm, [OH-PDMS] : [PDMOS] : [**1**] = 1-x : x : 0.02 (weight ratio) in plot A, [OH-PDMS]: [PDMOS] : [**2**] : [BP] : [TPP] = 1-x : x : 0.02 : 0.02 : 0.02 in plot B, 25°C, Hg-Xe lamp, 200 mW/cm^2, 5 min. [Color figure can be viewed in the online issue, which is available at wileyonlinelibrary.com.]

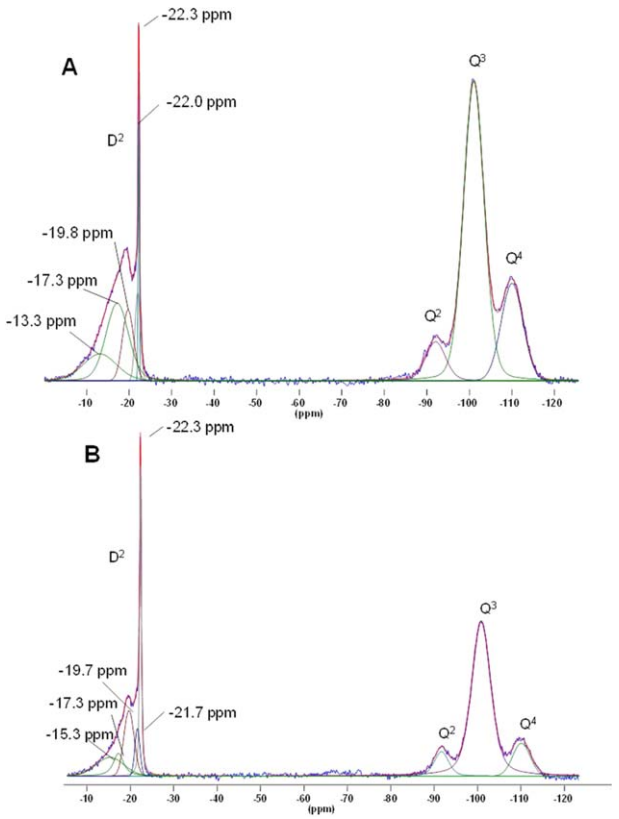

Figure 4. Si CP-MAS NMR spectra of the OH-PDMS/PDMOS (50/50 wt %) films prepared under photoacid (A) and photobase (B) conditions. Film thickness = 5 μm, [OH-PDMS] : [PDMOS] : [**1**] = 0.5 : 0.5 : 0.02 (weight fraction) in plot A, [OH-PDMS] : [PDMOS] : [**2**] : [BP] : [TPP] = 0.5 : 0.5 : 0.02 : 0.02 : 0.02 in plot B, 25°C, UV conveyor, H lamp, 1.46 J/cm^2/pass, 10 passes. [Color figure can be viewed in the online issue, which is available at wileyonlinelibrary.com.]

provided through the use of RT-FTIR to visualize the quantitative hydrolysis of the methoxysilyl functions of PDMOS. For this, we quantified the absorbance decrease of the CH_3 symmetric stretching vibration band (2848 cm^{-1}) arising from the $SiOCH_3$ groups. Regardless of the type of catalyst, the methoxysilyl conversion-time curves in Figure 3 revealed a complete hydrolysis with a limited impact of PDMOS content on the kinetic profiles. In addition, the kinetic data demonstrated again the faster cure rates under photoacid conditions compared with photobase conditions.

Cross-Linked Siloxane Microstructure. A question needs to be posed regarding the hybrid siloxane network determined by the ratio of homo- or hetero-condensation reactions between OH-PDMS and PDMOS oligomers. Using ^{29}Si solid-state NMR, the polysiloxane structures which arise from the two siloxane derivatives can be distinguished, and described respectively in terms of D and Q notations.[25] In the absence of UV irradiation, the OH-PDMS has a $D^1(D^2)_nD^1$ disilanol linear structure containing D^2 disiloxane species ($Me_2Si(OSi)_2$) in the chain backbone, and D^1 monosiloxane species ($HOSi(Me)_2(OSi)$) in terminal positions (see Figure S3 for the ^{29}Si liquid state NMR spectrum of the OH-PDMS oligomer).[26] Figure 4 compares the ^{29}Si CP-

MAS NMR spectra of two OH-PDMS films containing 50 wt. % PDMOS ($x = 0.50$) under photoacid and photobase conditions. Confirmation of cross-linker condensation was given by the triplet of Q^2, Q^3, and Q^4 units ($Si(OH)_{n-4}(OSi)_n$, n = 2 - 4) around −100 ppm straightforwardly assigned to cross-linked PDMOS. Q^3 was the dominant species in both cases, but the proportion of tetrasiloxane species (Q^4) was more prominent with **1** (17 %) compared to **2** (11 %). It was noted also, that the resultant hybrid films were less condensed than their inorganic analogues obtained through the photopolymerization of PDMOS alone ($x = 1$). In this latter case, Q^4 species accounted for 48 % (**1**) and 26 % (**2**) of the total silicate.

In addition, a broad D^2 signal at ca. −20 ppm indicated in both conditions the incorporation of OH-PDMS.[27,28] In an attempt to shed light into the silicate speciation arising from the PDMS segments, a deconvolution of the D^2 massif was performed. Although it was not unique, our best deconvolution revealed five distinct peaks displaying an increasing linewidth as the chemical shifts increased. The major feature of this portion of the ^{29}Si spectrum could be understood in terms of a diminished mobility causing the D^2 resonance to shift toward more positive values and become broader. For the photoacid-catalyzed system [Figure 4(A)], the two sharp components at −22.3 ppm and −22.0 ppm were thus attributed to D^2 silicon units in a mobile environment and presumably localized in the PDMS chain interior ($(D^2)_x$-D^2-$(D^2)_y$). According to Babonneau et al.,[29] their occurrence might appear as the indirect evidence of homopolymerization between OH-PDMS chains affording longer linear chains. By contrast, the three broader D signals at −19.8 ppm, −17.3 ppm, and −13.3 ppm reflected a more rigid environment arising for a closer proximity of cross-linked Q^n neighbors. Additionally, their breath is due to the overlap of a large number of single resonance lines produced as a result of the highly varied environments of the silicon nuclei. Depending on the proximity with Q species and their extent of condensation (Q^2-Q^4), both the environment and rigidity of the D^2 silicon sites change, resulting in very broad linewidths. The more downfielded signal at −13.3 ppm was thus tentatively assigned to D^2 units directly attached to Q units (Q^n-D^2-$(D^2)_x$) while the intermediate broad signals might correspond to D^2 more distant of the Q units (Q^n-D^2-D^2-$(D^2)_x$). Knowing the exact attribution of D^2 species was obviously not possible, but the presence of these broad features was apparently consistent with hetero-condensation reactions between OH-PDMS and PDMOS. It was not possible to reliably resolve the presence of uncondensed D^1 species at −12 ppm initially visible in the OH-PDMS ^{29}Si spectrum (Figure S2). However, the absence at this chemical shift of narrow lines arising from these very mobile silicon nuclei argued for an extended condensation of the terminal silanols. Clearly, our interpretation can be extended to the NMR spectrum of the photobase-catalyzed film [Figure 4(B)] displaying also five deconvoluted peaks in the D^2 region with only slight variations in their maxima position. By comparing PAG and PBG-mediated systems, we found that the nature of the photocatalyst had also an effect on the shape of the D^2 resonance. Thus, the proportion in sharp resonances (−22.3 and −21.7 ppm) was significantly enhanced in the photobase-catalyzed system, suggesting a decrease in the number of chemical linkages between OH-PDMS and the Q polysiloxane network. Accordingly, a faster homocondensation between OH-PDMS oligomers is presumably favored under base conditions.[30]

CONCLUSIONS

We have demonstrated the use of diaryl iodonium salt and α-aminoacetophenone as effective photoacid and photobase catalysts for the cross-linking of α,ω-silanol terminated silicone oligomers in presence of polydimethoxysiloxane cross-linker. By excluding metal and solvent, these two different pathways arise as facile and attractive alternatives to conventional polycondensation. Regardless of the photocatalyst employed, our synthetic methodology is "one pot" taking place within minutes at low organocatalyst loading. Faster photoacid-mediated cross-linking kinetics were recorded *in situ* through the use of rapid scan IR spectroscopy techniques. Additionally, the siloxane microstructure was characterized in detail by ^{29}Si solid-state NMR with a focus on the parameters promoting hetero-condensation reactions between OH-PDMS chains and the cross-linking agent PDMOS. Obviously, the resulting material might be of particular interest for applications in which metal residues are problematic. Furthermore the synthetic simplicity and the photolatency make them attractive in films used for local repair and applications requiring very fast cross-linking. Furthermore, the employment of these organic photocatalysts is an attractive and efficient alternative to organometallic catalysts.

REFERENCES

1. Heilen, W. Silicone Resins and Their Combinations; Vincentz Network: Hannover, **2005**.
2. Brook, M. A. Silicon in Organic, Organometallic, and Polymer Chemistry; Wiley: New York, **2000**.
3. Clarson, S. J.; Semlyen, J. A. Siloxane Polymers; Prentice Hall PTR: Englewood Cliffs, USA, **1993**.
4. Noll, W. J. Chemistry and Technology of Silicones Academic Press: New York, **1968**.
5. Brook, M. A. Silicon in Organic, Organometallic, and Polymer Chemistry; Wiley, Inc. 2000. United States, **2000**.
6. Cervantes, J.; Zarraga, R.; Salazar-Hernandez, C. *Appl. Organomet. Chem.* **2012**, *26*, 157.
7. Fawcett, A. S.; Grande, J. B.; Brook, M. A. *J. Polym. Sci., Part A: Polym. Chem.* **2013**, *51*, 644.
8. Kunzler, J. F. *Trends Polymer Sci.* **1996**, *4*, 52.
9. Crivello, J. V. *J. Polym. Sci., Part A: Polym. Chem.* **1999**, *37*, 4241.
10. Suyama, K.; Shirai, M. *Prog. Polym. Sci.* **2009**, *34*, 194.
11. Fouassier, J. P.; Lalevée, J. Photoinitiators for Polymer Synthesis: Scope, Reactivy and Efficiency; Wiley-VCH: Weinheim, Germany, **2012**.
12. Versace, D.-L.; Chemtob, A.; Croutxé-Barghorn, C.; Rigolet, S. *Macromol. Mater. Eng.* **2010**, *295*, 355.
13. Chemtob, A.; Courtecuisse, F.; Croutxe-Barghorn, C.; Rigolet, S. *New J. Chem.* **2011**, *35*, 1803.

14. Kura, H.; Oka, H.; Birbaum, J. L.; Kikuchi, T. *J. Photopolym. Sci. Tech.* **2000**, *13*, 145.

15. Dietliker, K.; Husler, R.; Birbaum, J. L.; Ilg, S.; Villeneuve, S.; Studer, K.; Jung, T.; Benkhoff, J.; Kura, H.; Matsumoto, A.; Oka, H. *Prog. Org. Coat.* **2007**, *58*, 146.

16. Muller, U.; Jockusch, S.; Timpe, H. J. *J. Polym. Sci., Part A: Polym. Chem.* **1992**, *30*, 2755.

17. Pyun, S. Y.; Kim, W. G. *Macromol. Res.* **2003**, *11*, 202.

18. Vazquez, C. P.; Tayouo, R.; Joly-Duhamel, C.; Boutevin, B. *J. Polym. Sci., Part A: Polym. Chem.* **2010**, *48*, 2123.

19. Campos, L. M.; Truong, T. T.; Shim, D. E.; Dimitriou, M. D.; Shir, D.; Meinel, I.; Gerbec, J. A.; Hahn, H. T.; Rogers, J. A.; Hawker, C. J.; *Chem. Mater.* **2009**, *21*, 5319.

20. De Paz, H.; Chemtob, A.; Croutxe-Barghorn, C.; Le Nouen, S.; Rigolet, S. *J. Phys. Chem. B* **2012**, *116*, 5260.

21. Massiot, D.; Fayon, F.; Capron, M.; King, I.; Le Calvé, S.; Alonso, B.; Durand, J.-O.; Bujoli, B.; Gan, Z.; Hoatson, G. *Magn. Reson. Chem.* **2002**, *40*, 70.

22. Colthup, N. B.; Daly, L. H.; Wiberley, S. E. Introduction to Infrared and Raman Spectroscopy; Academic Press, **1990**.

23. C. Belon, X. Allonas, C. Croutxé-Barghorn, J. Lalevée, *J. Polym. Sci., Part A: Polym. Chem.* **2010**, *48*, 2462.

24. Chemtob, A.; De Paz-Simon, H.; Croutxé-Barghorn, C.; Allonas, X.; Vidal, L.; Rigolet, S. *Thin Solid Films* **2013**, Submitted.

25. Brinker, C. J.; Scherer, G. W. Sol-Gel Science; Academic Press: San Diego, **1990**.

26. Rankin, S. E.; McCormick, A. V. *Magn. Res. Chem.* **1999**, *37*, S27.

27. Salinas, A. J.; Merino, J. M.; Babonneau, F.; Gil, F. J.; Vallet-Regi, M. *J. Biomed. Mater. Res. B* **2007**, *81B*, 274.

28. Tsuru, K.; Aburatani, Y.; Yabuta, T.; Hayakawa, S.; Ohtsuki, C.; Osaka, A. *J. Sol-Gel Sci. Technol.* **2001**, *21*, 89.

29. Babonneau, F. *New J. Chem.* **1994**, *18*, 1065.

30. Brinker, C. J. *J. Non-Cryst. Solids* **1988**, *100*, 31.